Spontaneous Dissolution of Ultralong Single- and Multiwalled Carbon Nanotubes

A. Nicholas G. Parra-Vasquez,[†,⊥,¶] Natnael Behabtu,[†,⊥] Micah J. Green,[†,⊥,#] Cary L. Pint,[‡,⊥] Colin C. Young,[⊥] Judith Schmidt,[∥] Ellina Kesselman,[∥] Anubha Goyal,[§] Pulickel M. Ajayan,[§] Yachin Cohen,[∥] Yeshayahu Talmon,[∥] Robert H. Hauge,[‡,⊥] and Matteo Pasquali[†,‡,⊥,*]

[†]Department of Chemical and Biomolecular Engineering, [‡]Department of Chemistry, [§]Department of Mechanical Engineering and Materials Science, and [⊥]The Richard E. Smalley Institute for Nanoscale Science and Technology, Rice University, 6100 Main Street, Houston, Texas 77005, and [∥]Department of Chemical Engineering, Technion-Israel Institute of Technology, Haifa 32000, Israel. [¶]Current address: Centre de Physique Moléculaire Optique et Hertzienne, Université de Bordeaux 1, F-33405 Talence, France. [#]Current address: Department of Chemical Engineering, Texas Tech University, Lubbock, Texas 79409.

ABSTRACT We report that chlorosulfonic acid is a true solvent for a wide range of carbon nanotubes (CNTs), including single-walled (SWNTs), double-walled (DWNTs), multiwalled carbon nanotubes (MWNTs), and CNTs hundreds of micrometers long. The CNTs dissolve as individuals at low concentrations, as determined by cryo-TEM (cryogenic transmission electron microscopy), and form liquid-crystalline phases at high concentrations. The mechanism of dissolution is electrostatic stabilization through reversible protonation of the CNT side walls, as previously established for SWNTs. CNTs with highly defective side walls do not protonate sufficiently and, hence, do not dissolve. The dissolution and liquid-crystallinity of ultralong CNTs are critical advances in the liquid-phase processing of macroscopic CNT-based materials, such as fibers and films.

KEYWORDS: carbon nanotubes · solubility · liquid crystals · long nanotubes · nanotube carpets · VACNT · SWNT · MWNT · DWNT · CNT · cryo-TEM

Carbon nanotubes (CNTs) are the subject of research in many scientific areas, including biological sensing, diagnosis, and cell ablation,[1−4] polymer property enhancement through reinforcement and improved conductivity,[5,6] and nanoscale electronics.[7−10] Carbon nanotubes occur as both single-walled (SWNTs) and multiwalled (MWNTs). One of the most significant limitations that prevents their use in wide scale applications is the difficulty in dispersing CNTs to form stable solutions, free of aggregates or bundles. Strong van der Waals forces (0.5 eV/nm for SWNTs[11]) cause CNTs to bundle; dissolution is increasingly difficult for long (>50 μm) pristine[12−15] CNTs. In some applications, CNTs must retain their individual optical signatures in solution.[3,16] In other applications, the CNT solution is only a processing step for making macroscopic materials, and the solvent is removed at the end of the process. For example, in the manufacturing of fibers and films, the goal is to retain CNT electronic and mechanical properties in the final product; ideally, such a final product would consist of a solid, ordered material made solely of CNTs. Of course, long CNTs can also be converted into fibers and films by solid-state processing; however, the final morphology (density and alignment) is not optimal, hindering the ultimate property of the macroscopic material. In contrast, liquid-phase processing combines optimal morphology with scalability.[17−22]

SWNTs have been dispersed using various techniques, through the use of either solvents,[23,24] wrapping agents (surfactants,[25,26] polymers,[27] or DNA[26,28]), or doping with alkali metals;[29] side wall functionalization broadens the range of concentrations and solvents available.[30−32] However, all of these methods have failed to achieve significant concentrations in liquid.[33,34] MWNTs are difficult to disperse in solvents unless they are oxidized,[35,36] functionalized,[37−39] wrapped,[40−42] or dispersed with a cosolvent.[43−45] Unlike SWNTs, oxidized MWNTs have been dispersed at high concentrations to produce liquid-crystalline solutions.[36] The concentrations achieved are high enough to produce films[46] and fibers,[47−49] but the products contain additives or functional groups that must be removed. This may be accomplished in part by complicating the process, such as with controlled heating or a series of washes; moreover, the removal of additives or functional groups creates voids in the assembled material.

Superacids (*e.g.*, fuming sulfuric and chlorosulfonic acids) dissolve HiPco SWNTs

*Address correspondence to mp@rice.edu.

Received for review April 23, 2010 and accepted June 17, 2010.

Published online July 1, 2010. 10.1021/nn100864v

at high concentrations (>10 wt %).[21,50−52] In the strongest of these, chlorosulfonic acid, SWNTs spontaneously disperse within minutes (movie M1 in Davis *et al.*[21]) and uniformly dissolve within an hour of stir-bar mixing.[53] Raman spectroscopy[21] and fluorescence[53] show that SWNTs maintain their integrity after being dissolved in acid, and that no oxidation occurs—unlike in mixtures of sulfuric and nitric acid.[54,55] Superacids dissolve SWNTs by reversibly protonating the surface of the SWNT with a delocalized positive charge; this charge induces a repulsive force between nanotubes and promotes dispersion by counteracting van der Waals attraction.[52] The fractional positive charge per carbon is measured by the change in the Raman shift of the G-peak;[52] Eklund *et al.* found a Raman shift of 320 cm^{-1} per hole per carbon.[56] The maximum isotropic concentration of HiPco SWNTs correlates with greater Raman shifts in G-peak; a minimal shift of 16 cm^{-1} in typical HiPco batches is needed to solubilize SWNTs enough to form liquid crystals.[21] From these high-concentration liquid-crystalline solutions (>10 wt %[21]), SWNTs can easily be processed into fibers and films.[51]

Macromolecules maximum isotropic concentration varies inversely with length; this relationship is well-established for polymers, as predicted by Flory and others,[57] and was recently extended to SWNTs.[58] For the same reasons, no solvents have been previously reported for long nanotubes (>50 μm). For pristine HiPco SWNTs (~1 μm), only superacids have been proven as solvents; SWNTs are weakly attractive in sulfuric acid and non-interacting or repulsive in chlorosulfonic acid.[21,58]

Here we show that chlorosulfonic acid dissolves a broad class of CNTs without damaging them. We measure the maximum isotropic concentration and liquid crystallinity in various CNT samples. We show that the dissolution, or solubility, of CNTs is related to the degree of carbon sp^2-hybridization on the CNT side walls, and that defect-free CNTs dissolve irrespective of length and type.

RESULTS AND DISCUSSION

Dissolution of Long SWNTs. We investigated the maximum isotropic concentration in sulfuric and chlorosulfonic acid of a wide variety of SWNTs produced by different methods: CoMoCat SWNTs, arc-discharge SWNTs, vertically aligned carpet-grown SWNTs, and CVD-grown SWNTs (Sunnano, CA). CoMoCat and arc-discharge SWNTs are similar in length to HiPco (0.5−2 μm), whereas Sunnano (~10 μm) and carpet SWNTs (10−100 μm) are longer, which makes dispersion more challenging.

In sulfuric acid, the maximum isotropic concentration for typical SWNT samples falls between 40 and 300 ppm, while ultralong SWNT samples showed no dispersion, only slight swelling. Minimal isotropic dispersion for long SWNTs is consistent with the previously established weak attractive forces between the SWNTs in sulfuric acid.[58] Such attractive forces applied over the full length of the long SWNTs coupled with far lower mobilities prevent the formation of any liquid-crystalline phase.

TABLE 1. Maximum Isotropic Concentration (MIC) of SWNTs in Chlorosulfonic Acid

CNT type	starting concn (ppm)	MIC (ppm)
HiPco SWNT	5000	4100
CoMoCat SWNT	5000	4200
arc-discharge SWNT	5000	2600
Sunnano SWNT	5000	450
Rice carpet SWNT	50[a]	>50

[a]Due to limited material availability, a sample was prepared at 50 ppm, centrifuged, and the concentration of SWNT remaining in solution was measured.

Upon addition of chlorosulfonic acid, each SWNT sample spontaneously turned homogeneously dark within minutes, where mixtures containing longer nanotubes become homogeneous more slowly. Raman measurements (Table S1 in the Supporting Information) show that all SWNT samples are protonated at levels similar to those of HiPco SWNTs, indicating that the mechanism of dissolution is indeed electrostatic repulsion due to protonation, quantified by the acid-induced change in the Raman G-peak. All SWNTs recover their Raman signatures when removed from chlorosulfonic acid; therefore, the SWNTs are not damaged by the acid (Figure S2 in the Supporting Information).

Table 1 reports the maximum isotropic concentration in the various SWNT samples, as measured by separating the denser liquid-crystalline phase (and any insoluble material) from the isotropic phase through centrifugation.[59] The concentration of the isotropic phase (supernatant) is measured by UV−vis−NIR absorption. CoMoCat and HiPco SWNTs have nearly identical maximum isotropic concentrations. Arc-discharge nanotubes have a slightly lower maximum isotropic concentration; this small difference is due to slightly longer SWNTs and a greater amount of impurities. For rigid rods in solution, the transition concentration from isotropic to biphasic is inversely proportional to aspect ratio (L/D).[60] Indeed, in samples of Sunnano SWNTs (higher aspect ratio), the concentration of the isotropic phase is 1 order of magnitude lower than in samples of shorter SWNTs (HiPco, CoMoCat, and arc-discharge). Carpet-grown SWNTs (L = 100 μm, $D \approx$ 3.2 nm) in chlorosulfonic acid approximate an ideal, nearly monodisperse system in an athermal solvent,[21] for which Onsager[60] predicts that the isotropic phase should be stable up to a concentration of $C^* = 3.34D/L \approx 100$ ppm. In fact, 50 ppm solutions of carpet-grown SWNTs are completely soluble and yield an isotropic phase; thus, the maximum isotropic concentration is expected to be greater than 50 ppm.

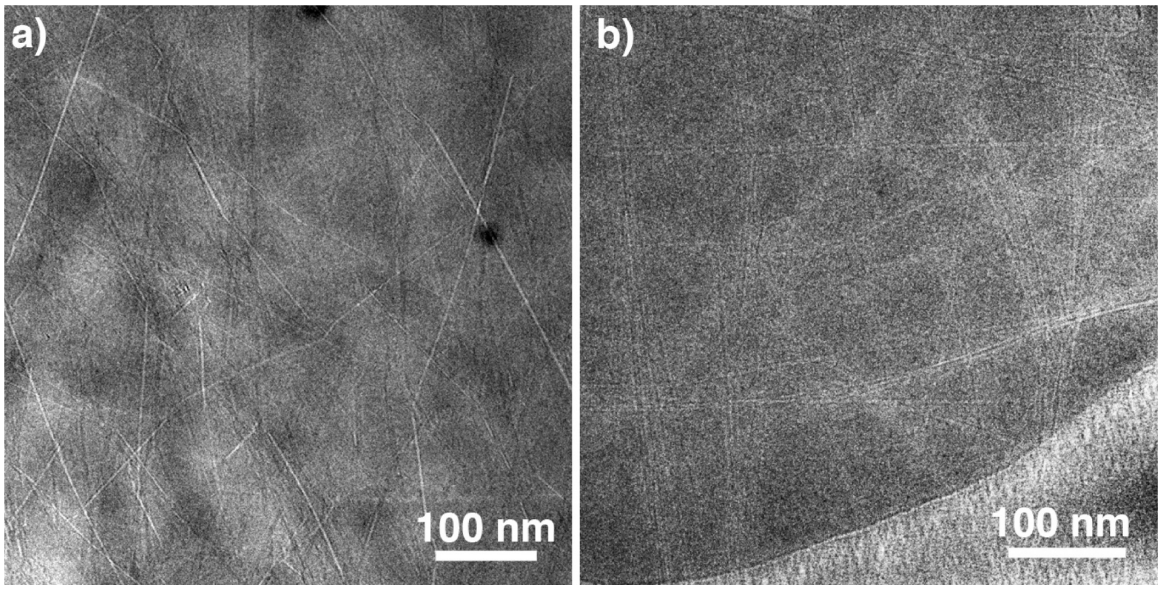

Figure 1. Cryo-TEM images of (a) carpet-grown SWNTs and (b) Sunnano SWNTs dispersed in chlorosulfonic acid reveal SWNTs dispersed as individuals. The vitrified chlorosulfonic acid has a higher electron density than the SWNTs. The concentrations are 100 and 300 ppm by mass, respectively.

Cryogenic transmission electron microscopy (cryo-TEM) is the best technique for determining the morphology of dilute phases of CNT-laden fluids;[16,21,25,61,62] moreover, it is the only reliable technique available for acid samples. Cryo-TEM images show clearly that carpet-grown and Sunnano SWNTs are dissolved as individuals in chlorosulfonic acid (Figure 1a,b, respectively). The images show no evidence of bundling or entanglement.

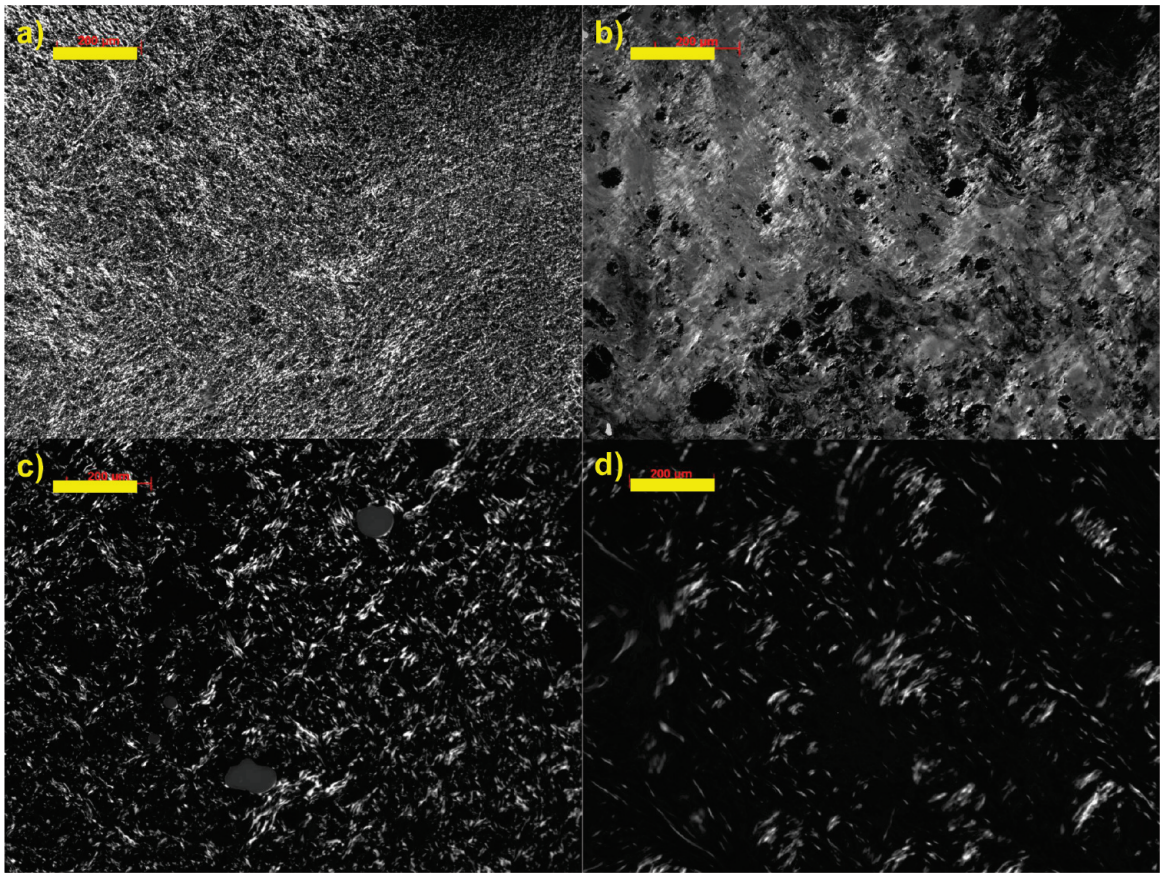

Figure 2. Bright-field light microscopy images of different types of SWNTs in chlorosulfonic acid: (a) HiPco (dispersed at 8 wt %), (b) CoMoCat (dispersed at 6 wt %), (c) arc-discharge (dispersed at 6 wt %), and (d) Sunnano (dispersed at 6 wt %). All images are viewed under cross-polarized light at 10×; since the polarized light is crossed at 0°, the liquid-crystalline domains oriented at ±45° are highlighted. All scale bars are 200 μm.

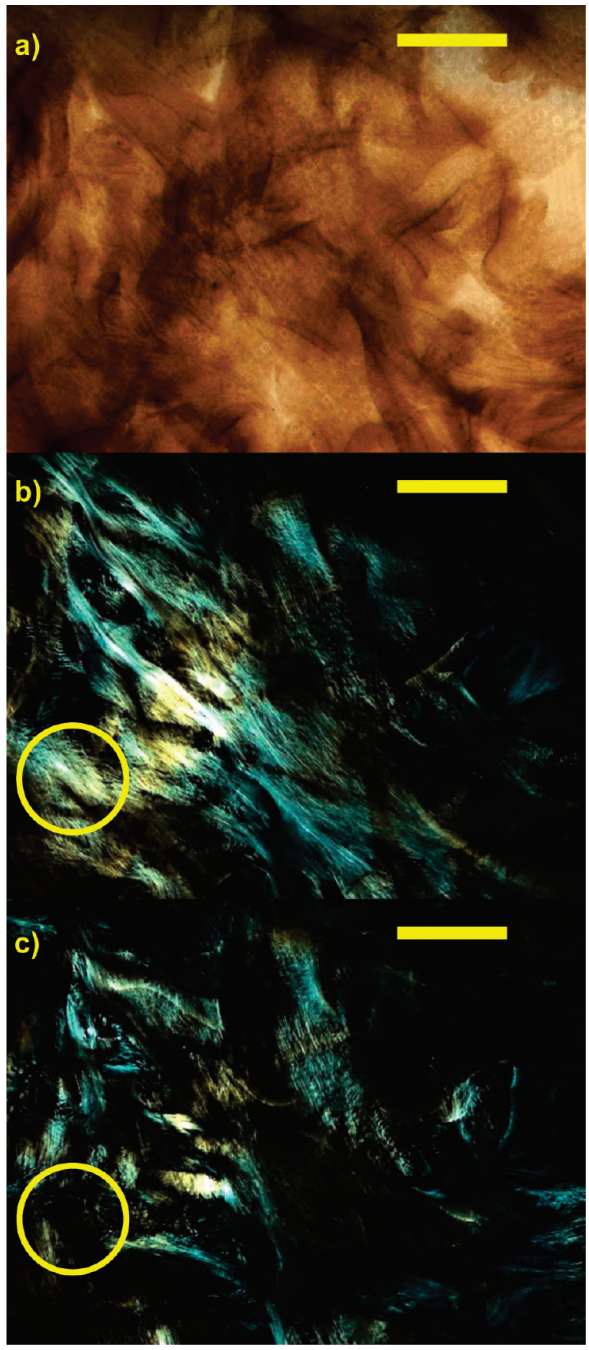

Figure 3. Color bright-field light microscopy images of concentrated carpet-grown SWNTs in chlorosulfonic acid. At this concentration, almost all SWNTs are dispersed, and the sample is in the biphasic region. Image (a) is viewed under nonpolarized light, while images (b) and (c) are viewed with cross-polarized light positioned at 0 and 45°, respectively, revealing highly birefringent liquid-crystalline domains. The LC domain circled (in b and c) is highlighted when the cross-polars are aligned at 0° (b), and dark when the cross-polars are aligned 45° (c). All scale bars correspond to 200 μm.

At high concentrations, HiPco (short) SWNTs form liquid crystals.[21] However, it has been long assumed that long SWNTs could never form a liquid-crystalline (LC) phase due to both difficulty in dispersion and entanglement and jamming during organization (similar to the occurrence of an isotropic gel phase in high molecular weight rod-like polymers).[63] Figures 2 and 3 show that, at high concentration, all of the SWNT samples, including ultralong SWNTs, display LC birefringence under cross-polarized light. Images in Figure 2 were acquired with the analyzer oriented at 0° and polarizer at 90°, hereafter referred to as cross-polarized light; thus, the brightest domains have an orientation at ±45°, whereas domains oriented parallel to the polarizer or analyzer appear dark. When the analyzer and polarizer are rotated by 45° (remaining fully crossed), LC domains oriented at ±45° turn dark, while previously dark domains turn bright. In both analyzer and polarizer configurations, isotropic dispersions, bubbles, and undispersed particles also appear dark (also see Figures S3−S6 in the Supporting Information). The LC domains from carpet-grown SWNTS (Figure 3) are larger than those made with any of the other SWNTs (Figure 2). The carpet-grown SWNTs form larger LC domains because of a combination of their pre-existing order and their greater lengths. Due to limited material availability, the ultralong SWNTs were mixed at a concentration in the biphasic chimney; thus, isotropic regions are still present in Figure 3a, which remain dark when viewed under cross-polarized light (Figure 3b,c). As an example of strong birefringence, a bright LC domain (circled in Figure 3b) turns completely dark (circled in Figure 3c) when the analyzer and polarizer are rotated by 45°.

Dissolution of MWNTs. The solubility of MWNTs in strong acids had not been studied before. Here we tested MWNTs with various diameters and number of walls:

(1) Rice carpet-grown DWNTs with small diameters (~2−3 nm), two walls, few defects, and intermediate lengths (50 ± 10 μm)
(2) Sunnano MWNTs, intermediate diameters (3−10 nm), few walls (<10), and intermediate lengths (10−30 μm)
(3) Rice carpet-grown MWNTs with intermediate diameters (5−15 nm), few walls (<10), few defects, and ultralong lengths (500 μm)

All of these MWNTs formed excellent dispersions in chlorosulfonic acid. Raman spectroscopy shows that, like SWNTs,[53] MWNTs are protonated in acid (Table S1 in the Supporting Information) and are not damaged by the acid (Figure S4). Cryo-TEM images indicate that the nanotubes are indeed dispersed as individuals (Figure 4).

The MWNTs dispersed in chlorosulfonic acid form LC phases at high concentrations. Light microscopy images of DWNTs (Figure 5a) showed no undispersed material and highly birefringent LC domains (also see Figure S8 in the Supporting Information). Carpet-grown, few-walled MWNTs (Figure 5b) showed a mixture of undispersed material and liquid-crystalline regions (also see Figure S9). The undispersed material does not affect LC formation because the MWNTs have pre-existing alignment; thus, they need little rearrangement to form LC domains. Intriguingly, few-walled Sunnano MWNTs showed no liquid crystallinity, even when the superna-

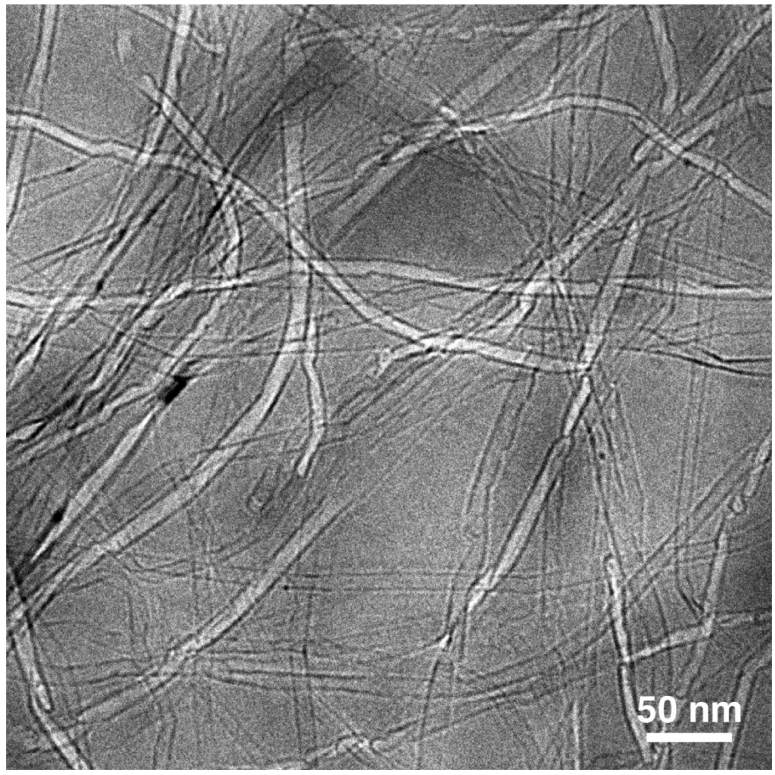

Figure 4. Cryo-TEM images of carpet-grown MWNTs dispersed in chlorosulfonic acid at 50 ppm by mass reveal MWNTs dispersed as individuals.

tant (free of insoluble material) was concentrated. TEM images of the supernatant revealed a high concentration of soluble highly curved, CNTs that do not display liquid crystallinity (Figure S10).

Table 2 shows the maximum isotropic concentration of MWNTs in chlorosulfonic acid; samples were measured by the same technique used for SWNTs.[59] The Rice carpet-grown MWNTs have a lower maximum isotropic concentration of 66 ppm because they are 500 μm in length and should transform from the isotropic to biphasic region at lower concentrations.

Effects of Defect Density. In CNTs, side wall protonation is highly dependent on the inherent ability of the structure to share electrons.[52,64] Therefore, any changes that disrupt the electrical properties of the CNTs, such as defects, will affect the ability of the CNT to be protonated. The disorder peak (D-peak) in Raman spectroscopy measures any defects that break the symmetry and perfection of the sp^2-hybridized π-cloud, such as functionalization, kinks, Stone-Wales defects, and sp^3-hybridization.[65]

To verify this hypothesis, three carpets were grown at different lengths and different degrees of disorder.

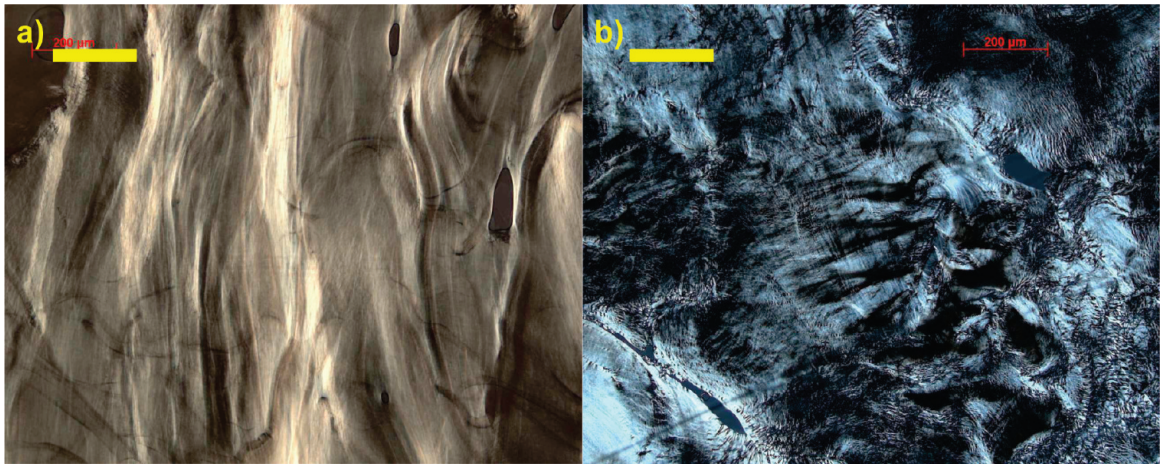

Figure 5. Bright-field, color light microscopy images of concentrated (a) carpet-grown DWNTs and (b) carpet-grown MWNTs in chlorosulfonic acid. At this concentration, mostly all DWNTs are dispersed and the sample is in the biphasic region. Images (a) and (b) are viewed with cross-polarized light positioned at 45 and 0°, respectively, revealing highly birefringent liquid-crystalline domains. Both images are at 10×, and the scale bars are 200 μm.

TABLE 2. Maximum Isotropic Concentration (MIC) of MWNTs in Chlorosulfonic Acid

CNT type	starting concn (ppm)	MIC (ppm)
Sunnano MWNT (D = 3−10 nm, L = 10−30 μm)	6000	4900
Rice carpet MWNT (D = 5−15 nm, L = 500 μm)	160[a]	66

[a]Due to limited material availability, a sample was prepared at 160 ppm, centrifuged, and the concentration of MWNT remaining in solution was measured.

Two carpets were grown at 750 °C for 15 and 30 min to produce low-defect SWNTs of 60 and 100 μm, respectively. A third carpet was grown at 550 °C for 30 min to produce a highly defective CNT sample (SWNT and few-walled MWNT) of 16 μm. Figure 6 shows the Raman spectra of the three samples; the highly defective SWNTs have a D/G (defect/pristine) ratio of 1 (Figure 6b), whereas the low-defect SWNTs have a D/G ratio of 0.2 (Figure 6a,c). Upon addition of chlorosulfonic acid, the low-defect SWNTs spontaneously dissolved, while the high-defect CNTs expanded and slightly exfoliated but did not dissolve. Figure 6 shows that, after 24 h of centrifugation, the low-defect SWNTs remained in solution irrespective of length, whereas the high-defect CNTs precipitated out of solution. We conclude that the solubilty of CNTs in chlorosulfonic acid varies inversely with defect density.

We note that the use of centrifugation to measure the maximum isotropic concentration of CNTs in chlorosulfonic acid needs to be studied further. We tested Mitsui MWNTs, which have large diameters (50−100 nm), many walls (>15), and few defects. The MWNTs visually dispersed when mixed with a stir bar (Figure S7 in the Supporting Information), and Raman analysis shows that they are protonated (Table S1) with a shift in G-peak of 22 cm^{-1}, similar to other high-quality CNTs protonated by chlorosulfonic acid. The G-peak shift and the uniform, spontaneous dispersion suggests that they are protonated enough to be electrostatically stable in solution. However, when centrifuged at 5000 rpm (~300g) for 8 h, they settle. Of course, strong enough centrifugation can precipitate molecules out of solution even if there is only a minimal difference between the density of the solvent and the molecule.[66−68] For example, ultracentrifugation has been applied to separate individual SWNTs by diameter[69] and length.[70−72] In the case of CNTs in acid, an estimation of the relative density of the CNTs with acid is complicated because the acid can fill (fully or partially) the CNTs, and this mechanism is still poorly documented

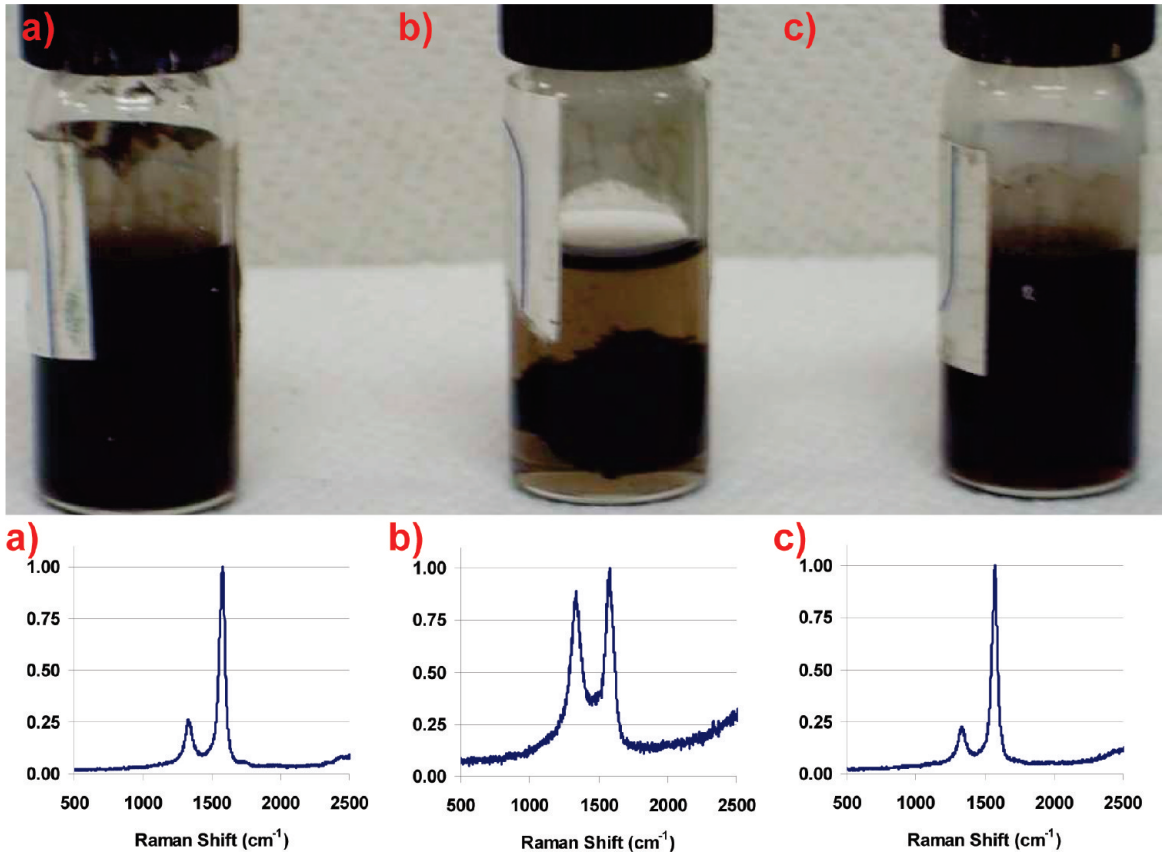

Figure 6. Solubility of carpet-grown CNTs shows strong dependence on nanotube defect density and weak dependence on nanotube length. Images (a) and (c) have minimal defects, and although they differ in length (60 and 100 μm), they are both soluble. However, image (b), grown with large amounts of defects (16 μm), is insoluble (slight discoloration). A measure of their defect density is shown by the intensity of the D-peak (1350 cm^{-1}) normalized to the G-peak (1590 cm^{-1}) in the Raman plots below each image; sp^3-hybridized carbons scale with the height of the D-peak.

and understood.[21,53,73] The size of MWNTs does not affect the solubility but the stability when centrifuged (see Supporting Information).

CONCLUSIONS

Dispersions of CNTs at high concentrations has been an extremely difficult task until now; we have shown that chlorosulfonic acid is the ultimate CNT solvent, and it has been recently extended to graphite.[74] CNTs produced by various techniques dissolve at concentrations above 0.25 wt %. Cryo-TEM demonstrates clearly that the CNTs are dispersed as individuals. At high concentrations, all low-defect rod-like CNT samples form liquid-crystalline domains, some having undispersed material present. Highly defective CNTs do not protonate sufficiently to dissolve in chlorosulfonic acid. Amazingly, both 100 μm SWNTs and 500 μm MWNTs spontaneously dissolve in chlorosulfonic acid and form liquid-crystalline domains. Both strength and conductivity of CNT fibers and films scale with the length of constituent CNTs;[15,75] therefore, the discovery that CNTs with high-quality side walls and near-millimeter length dissolve in chlorosulfonic acid opens the route for scalable fluid processing of CNT fibers and films with commercially viable macroscopic properties.

METHODS

Materials. Carbon nanotubes were produced by several manufacturers. Single-walled nanotubes (SWNTs) utilized in this study were CoMoCat SWNTs (produced by SWeNT, SG65 freeze-dried powder, lot # 000-0025), HiPco SWNTs (produced at Rice University, batch 188.3, diameters = 0.7 to 1.4 nm,[76] lengths = 100 nm to 3 μm[77]), carpet-grown SWNTs (produced at Rice University, diameters = 0.8 to 4 nm[14]), arc-discharge SWNTs (produced by Carbon Solutions, Inc., p2-SWNTs, batch # 02-304), and CVD grown Sunnano SWNTs (produced by Sun Innovations, Inc., lot # SN2102). Multiwalled nanotubes (MWNTs) were obtained from Mitsui & Co, Ltd. (lot # 05072001k28), Rice University (carpet-grown MWNT, diameters = 5 to 15 nm), and Sun Innovations, Inc. (CVD growth, Sunnano MWNT). Carpets of SWNTs were made at Rice University by depositing catalyst through e-beam evaporation of a 0.5/10 nm Fe/Al_2O_3 film on SiO_2 and using acetylene as the carbon source in a water-assisted CVD technique with three different procedures: grown at 750 °C for 15 min (60 μm), grown at 750 °C for 30 min (100 μm), and grown at 550 °C for 15 min (16 μm).[14,78] Carpets of primarily DWNTs were prepared using a similar method, except with growth at 675 °C. Unlike lower growth temperatures that lead to highly defective material with many walls, this condition gives relatively pristine CNTs that have mostly two walls.[78] Carpets of MWNTs made at Rice University were prepared by a similar method to the SWNT carpets: 1−3/5−20 nm Fe/Al_2O_3 film was evaporated onto SiO_2 wafer and then heated at 750−800 °C. MWNTs were grown to a height of 500 μm on average using ethylene as the carbon source in a water-assisted CVD technique.[79] All carpet lengths were measured by SEM.

ACS-certified chlorosulfonic acid (density = 1753 kg/m^3) was used as received from Sigma Aldrich. All chemicals, unless otherwise noted, were purchased from Sigma Aldrich (St. Louis, MO) and were used without further purification.

Maximum Isotropic Concentration Measurements. When sufficient quantities (20 mg) of the CNTs could be procured, a biphasic solution was centrifuged at 5000 rpm (~300*g*) to separate the isotropic phase in equilibrium with the nematic phase; both phases are CNT solutions. The maximum isotropic concentration is the concentration of the supernatant, determined by UV−vis−NIR spectroscopy.[59] When the starting material was insufficient to produce a high-concentration biphasic solution, concentrations were prepared at 160 and 50 mg/L and centrifuged for 12 h to check whether CNTs remain in solution.

Raman Measurements. Concentrated solutions of SWNTs in chlorosulfonic acid (between 0.5 and 2 wt %) were prepared for microscopic examination by mixing with a stir bar in a glovebox (dew point −50 °C) and then were hermetically sealed with aluminum tape between a dry microscope slide and a glass coverslip. Two different dry samples were prepared for Raman analysis. The starting material was placed onto double-sided scotch tape on a glass slide; for comparison, CNTs were quenched from chlorosulfonic acid into ether and filtered to form a bucky paper that was placed on a glass slide. The samples were examined by polarized Raman spectroscopy in the reflection geometry employing a Renishaw micro-Raman spectrometer. Two different lasers at excitation wavelengths of 514 nm (Ar^+ ion) and 785 nm (diode) were used.

Cryo-Transmission Electron Microscopy. CNTs (HiPco SWNTs, carpet-grown SWNTs, Sunnano SWNTs, and carpet-grown MWNTs) were dispersed in 97% reagent grade chlorosulfonic acid at low concentrations (50−300 ppm by mass). Dispersions were prepared and mixed for a day in a dry glovebox. Two milliliters of solution was transferred to a small vial and placed in the vitrification apparatus along with a fiber glass filter paper and glass pipet. The entire setup was placed in a glovebag and purged with ultrapure nitrogen (99.9995%) for 30 min. A drop of the SWNT solution was then placed on 200 copper mesh, lacey carbon grid (Ted Pella). The fiber glass filter paper (unreactive with chlorosulfonic acid) was then used to blot the sample, leaving a thin film of liquid. The grid was then quickly vitrified in liquid nitrogen and placed in a cryo-specimen holder for transfer to the TEM. The samples were imaged in an FEI T12 G^2 transmission electron microscope operated at 120 kV, using a Gatan 626 cooling holder operated at about −180 °C. Images were recorded by a Gatan US1000 cooled CCD camera.

Light Microscopy. The concentrated samples that had been previously sealed for Raman characterization were subsequently examined by polarized light microscopy in a Zeiss Axioplan 2 polarized light microscope equipped with an oil immersion objective (63×, 1.4 NA) and a rotatable sample holder mounted between the polarizer and analyzer. To allow sufficient light transmission, the sample was thinned by squeezing the coverslip and the slide.

Transmission Electron Microscopy. Room temperature TEM microscopy was performed on quenched samples mixed with styrene and bath sonicated for 5 min to break up large bundles. Five microliters of the mixture was pipetted onto a 300 mesh, lacey carbon grid (Ted Pella), blotted on the back side with a filter paper, and then placed in a vacuum oven at 60 °C overnight. The samples were then imaged in a JEOL 2100F FEG-TEM operated at 200 kV.

Acknowledgment. We gratefully acknowledge useful discussions with H. Schmidt, J. Lomeda, D. Tsentalovich, E. Haroz, and W. Adams. We also acknowledge M. Majumder and B. Dan for their help with film preparations and characterizations. We acknowledge E. Howland and D. Maher for their aid in characterizing the solutions. Funding was provided by AFOSR Grants FA9550-06-1-0207 and FA9550-09-1-0590, AFRL Agreements FA8650-07-2-5061 and 07-S568-0042-01-C1, NSF Division of Materials Research Grant 06090077, the Robert A. Welch Foundation (Grant C-1668), the United States−Israel Binational Science Foundation, and the Evans-Attwell Welch Postdoctoral Fellowship. Cryo-TEM imaging was performed at the Laboratory for Advanced Microscopy of Soft Matter, supported by the Technion Russell Berrie Nanotechnology Institute.

Supporting Information Available: Raman shifts in G-peak for CNTs dispersed in chlorosulfonic acid, Raman spectroscopy of SWNTs upon acid removal, micrographs of different CNTs forming a liquid-crystalline phase, images of dispersions of MWNTs, and sedimentation analysis. This material is available free of charge *via* the Internet at http://pubs.acs.org.

REFERENCES AND NOTES

1. Sinnott, S. B.; Andrews, R. Carbon Nanotubes: Synthesis, Properties, and Applications. *Crit. Rev. Solid State Mater. Sci.* **2001**, *26*, 145–249.
2. Dai, H. J. Carbon Nanotubes: Opportunities and Challenges. *Surf. Sci.* **2002**, *500*, 218–241.
3. Gannon, C. J.; Cherukuri, P.; Yakobson, B. I.; Cognet, L.; Kanzius, J. S.; Kittrell, C.; Weisman, R. B.; Pasquali, M.; Schmidt, H. K.; Smalley, R. E.; *et al.* Carbon Nanotube-Enhanced Thermal Destruction of Cancer Cells in a Noninvasive Radiofrequency Field. *Cancer* **2007**, *110*, 2654–2665.
4. Palwai, N. R.; Martyn, D. E.; Neves, L. F. F.; Tan, Y.; Resasco, D. E.; Harrison, R. G. Retention of Biological Activity and Near-Infrared Absorbance upon Adsorption of Horseradish Peroxidase on Single-Walled Carbon Nanotubes. *Nanotechnology* **2007**, *18*, 235601.
5. Andrews, R.; Jacques, D.; Rao, A. M.; Rantell, T.; Derbyshire, F.; Chen, Y.; Chen, J.; Haddon, R. C. Nanotube Composite Carbon Fibers. *Appl. Phys. Lett.* **1999**, *75*, 1329–1331.
6. Bryning, M. B.; Milkie, D. E.; Islam, M. F.; Kikkawa, J. M.; Yodh, A. G. Thermal Conductivity and Interfacial Resistance in Single-Wall Carbon Nanotube Epoxy Composites. *Appl. Phys. Lett.* **2005**, *87*, 161909.
7. Allen, B. L.; Kichambare, P. D.; Star, A. Carbon Nanotube Field-Effect-Transistor-Based Biosensors. *Adv. Mater.* **2007**, *19*, 1439–1451.
8. Appenzeller, J.; Martel, R.; Derycke, V.; Radosavjevic, M.; Wind, S.; Neumayer, D.; Avouris, P. Carbon Nanotubes as Potential Building Blocks for Future Nanoelectronics. *Microelectron. Eng.* **2002**, *64*, 391–397.
9. Choi, H. J.; Ihm, J.; Louie, S. G.; Cohen, M. L. Defects, Quasibound States, and Quantum Conductance in Metallic Carbon Nanotubes. *Phys. Rev. Lett.* **2000**, *84*, 2917–2920.
10. Johnston, D. E.; Islam, M. F.; Yodh, A. G.; Johnson, A. T. Electronic Devices Based on Purified Carbon Nanotubes Grown by High-Pressure Decomposition of Carbon Monoxide. *Nat. Mater.* **2005**, *4*, 589–592.
11. Girifalco, L. A.; Hodak, M.; Lee, R. S. Carbon Nanotubes, Buckyballs, Ropes, and a Universal Graphitic Potential. *Phys. Rev. B* **2000**, *62*, 13104–13110.
12. Ren, Z. F.; Huang, Z. P.; Xu, J. W.; Wang, J. H.; Bush, P.; Siegal, M. P.; Provencio, P. N. Synthesis of Large Arrays of Well-Aligned Carbon Nanotubes on Glass. *Science* **1998**, *282*, 1105–1107.
13. Fan, S. S.; Chapline, M. G.; Franklin, N. R.; Tombler, T. W.; Cassell, A. M.; Dai, H. J. Self-Oriented Regular Arrays of Carbon Nanotubes and Their Field Emission Properties. *Science* **1999**, *283*, 512–514.
14. Pint, C. L.; Pheasant, S. T.; Pasquali, M.; Coulter, K. E.; Schmidt, H. K.; Hauge, R. H. Synthesis of High Aspect-Ratio Carbon Nanotube "Flying Carpets" from Nanostructured Flake Substrates. *Nano Lett.* **2008**, *8*, 1879–1883.
15. Behabtu, N.; Green, M. J.; Pasquali, M. Carbon Nanotube-Based Neat Fibers. *Nano Today* **2008**, *3*, 24–34.
16. Duque, J. G.; Cognet, L.; Parra-Vasquez, A. N. G.; Nicholas, N.; Schmidt, H. K.; Pasquali, M. Stable Luminescence from Individual Carbon Nanotubes in Acidic, Basic, and Biological Environments. *J. Am. Chem. Soc.* **2008**, *130*, 2626–2633.
17. Yoshimura, M.; Suchanek, W. *In Situ* Fabrication of Morphology-Controlled Advanced Ceramic Materials by Soft Solution Processing. *Solid State Ionics* **1997**, *98*, 197–208.
18. Nguyen, T. Q.; Yee, R. Y.; Schwartz, B. J. Solution Processing of Conjugated Polymers: The Effects of Polymer Solubility on the Morphology and Electronic Properties of Semiconducting Polymer Films. *J. Photochem. Photobiol., A* **2001**, *144*, 21–30.
19. Guillemoles, J. F.; Connolly, J. P.; Ramdani, O.; Roussel, O.; Guimard, D.; Bermudez, V.; Naghavi, N.; Grand, P. P.; Parissi, L.; Kurdi, J.; *et al.* Solution Processing Route to High Efficiency CuIn(S, Se)(2) Solar Cells. *J. Nano Res.* **2008**, *4*, 79–89.
20. Byrappa, K. Novel Hydrothermal Solution Routes of Advanced High Melting Nanomaterials Processing. *J. Ceram. Soc. Jpn.* **2009**, *117*, 236–244.
21. Davis, V. A.; Parra-Vasquez, A. N. G.; Green, M. J.; Rai, P. K.; Behabtu, N.; Prieto, V.; Booker, R. D.; Schmidt, J.; Kesselman, E.; Zhou, W.; *et al.* True Solutions of Single-Walled Carbon Nanotubes for Assembly into Macroscopic Materials. *Nat. Nanotechnol.* **2009**, *4*, 830–834.
22. Tung, V. C.; Chen, L. M.; Allen, M. J.; Wassei, J. K.; Nelson, K.; Kaner, R. B.; Yang, Y. Low-Temperature Solution Processing of Graphene−Carbon Nanotube Hybrid Materials for High-Performance Transparent Conductors. *Nano Lett.* **2009**, *9*, 1949–1955.
23. Bahr, J. L.; Mickelson, E. T.; Bronikowski, M. J.; Smalley, R. E.; Tour, J. M. Dissolution of Small Diameter Single-Wall Carbon Nanotubes in Organic Solvents. *Chem. Commun.* **2001**, 193–194.
24. Bergin, S. D.; Nicolosi, V.; Streich, P. V.; Giordani, S.; Sun, Z.; Windle, A. H.; Ryan, P.; Niraj, P. P.; Wang, Z.-T.; Carpenter, L.; *et al.* Towards Solutions of Single-Walled Carbon Nanotubes in Common Solvents. *Adv. Mater.* **2008**, *20*, 1876–1881.
25. Moore, V. C.; Strano, M. S.; Haroz, E. H.; Hauge, R. H.; Smalley, R. E.; Schmidt, J.; Talmon, Y. Individually Suspended Single-Walled Carbon Nanotubes in Various Surfactants. *Nano Lett.* **2003**, *3*, 1379–1382.
26. Haggenmueller, R.; Rahatekar, S. S.; Fagan, J. A.; Chun, J. H.; Becker, M. L.; Naik, R. R.; Krauss, T.; Carlson, L.; Kadla, J. F.; Trulove, P. C.; *et al.* Comparison of the Quality of Aqueous Dispersions of Single Wall Carbon Nanotubes Using Surfactants and Biomolecules. *Langmuir* **2008**, *24*, 5070–5078.
27. O'Connell, M. J.; Boul, P.; Ericson, L. M.; Huffman, C.; Wang, Y. H.; Haroz, E.; Kuper, C.; Tour, J.; Ausman, K. D.; Smalley, R. E. Reversible Water-Solubilization of Single-Walled Carbon Nanotubes by Polymer Wrapping. *Chem. Phys. Lett.* **2001**, *342*, 265–271.
28. Zheng, M.; Jagota, A.; Strano, M. S.; Santos, A. P.; Barone, P.; Chou, S. G.; Diner, B. A.; Dresselhaus, M. S.; McLean, R. S.; Onoa, G. B.; *et al.* Structure-Based Carbon Nanotube Sorting by Sequence-Dependent DNA Assembly. *Science* **2003**, *302*, 1545–1548.
29. Penicaud, A.; Poulin, P.; Derre, A.; Anglaret, E.; Petit, P. Spontaneous Dissolution of a Single-Wall Carbon Nanotube Salt. *J. Am. Chem. Soc.* **2005**, *127*, 8–9.
30. Dyke, C. A.; Tour, J. M. Covalent Functionalization of Single-Walled Carbon Nanotubes for Materials Applications. *J. Phys. Chem. A* **2004**, *108*, 11151–11159.
31. Chen, Z. Y.; Kobashi, K.; Rauwald, U.; Booker, R.; Fan, H.; Hwang, W. F.; Tour, J. M. Soluble Ultra-Short Single-Walled Carbon Nanotubes. *J. Am. Chem. Soc.* **2006**, *128*, 10568–10571.
32. Nimmagadda, A.; Thurston, K.; Nollert, M. U.; McFetridge, P. S. F. Chemical Modification of SWNT Alters *In Vitro* Cell−SWNT Interactions. *J. Biomed. Mater. Res., Part A* **2006**, *76A*, 614–625.
33. Islam, M. F.; Rojas, E.; Bergey, D. M.; Johnson, A. T.; Yodh, A. G. High Weight Fraction Surfactant Solubilization of Single-Wall Carbon Nanotubes in Water. *Nano Lett.* **2003**, *3*, 269–273.
34. Badaire, S.; Zakri, C.; Maugey, M.; Derre, A.; Barisci, J. N.; Wallace, G.; Poulin, P. Liquid Crystals of DNA-Stabilized Carbon Nanotubes. *Adv. Mater.* **2005**, *17*, 1673.
35. Salam, M. A.; Burk, R. C. Thermodynamics of Pentachlorophenol Adsorption from Aqueous Solutions by Oxidized Multi-Walled Carbon Nanotubes. *App. Surf. Sci.* **2008**, *255*, 1975–1981.

36. Song, W. H.; Kinloch, I. A.; Windle, A. H. Nematic Liquid Crystallinity of Multiwall Carbon Nanotubes. *Science* **2003**, *302*, 1363.
37. Feng, W.; Zhou, F.; Wang, X. G.; Wan, M. X.; Fujii, A.; Yoshino, K. Water-Soluble Multi-Walled Nanotube and Its Film Characteristics. *Chin. Phys. Lett.* **2003**, *20*, 753–755.
38. Singh, R.; Pantarotto, D.; McCarthy, D.; Chaloin, O.; Hoebeke, J.; Partidos, C. D.; Briand, J. P.; Prato, M.; Bianco, A.; Kostarelos, K. Binding and Condensation of Plasmid DNA onto Functionalized Carbon Nanotubes: Toward the Construction of Nanotube-Based Gene Delivery Vectors. *J. Am. Chem. Soc.* **2005**, *127*, 4388–4396.
39. Klink, M.; Ritter, H. Supramolecular Gels Based on Multi-Walled Carbon Nanotubes Bearing Covalently Attached Cyclodextrin and Water-Soluble Guest Polymers. *Macromol. Rapid Commun.* **2008**, *29*, 1208–1211.
40. Sinani, V. A.; Gheith, M. K.; Yaroslavov, A. A.; Rakhnyanskaya, A. A.; Sun, K.; Mamedov, A. A.; Wicksted, J. P.; Kotov, N. A. Aqueous Dispersions of Single-Wall and Multiwall Carbon Nanotubes with Designed Amphiphilic Polycations. *J. Am. Chem. Soc.* **2005**, *127*, 3463–3472.
41. Hyung, H.; Fortner, J. D.; Hughes, J. B.; Kim, J. H. Natural Organic Matter Stabilizes Carbon Nanotubes in the Aqueous Phase. *Environ. Sci. Technol.* **2007**, *41*, 179–184.
42. Karousis, N.; Tsotsou, G. E.; Ragoussis, N.; Tagmatarchis, N. Catalytic Activity of Surfactant-Solubilized Multi-Walled Carbon Nanotubes Decorated with Palladium Nanoparticles. *Diamond Relat. Mater.* **2008**, *17*, 1582–1585.
43. Chun, K. Y.; Choi, S. K.; Kang, H. J.; Park, C. Y.; Lee, C. J. Highly Dispersed Multi-Walled Carbon Nanotubes in Ethanol Using Potassium Doping. *Carbon* **2006**, *44*, 1491–1495.
44. Chen, H.; Muthuraman, H.; Stokes, P.; Zou, J. H.; Liu, X.; Wang, J. H.; Huo, Q.; Khondaker, S. I.; Zhai, L. Dispersion of Carbon Nanotubes and Polymer Nanocomposite Fabrication Using Trifluoroacetic Acid as a Co-solvent. *Nanotechnology* **2007**, *18*, 415606.
45. Xie, X. F.; Gan, T.; Sun, D.; Wu, K. B. Application of Multi-Walled Carbon Nanotubes/Nafion Composite Film in Electrochemical Determination of Pb^{2+}. *Fullerenes, Nanotubes, Carbon Nanostruct.* **2008**, *16*, 103–113.
46. Dan, B.; Irvin, G. C.; Pasquali, M. Continuous and Scalable Fabrication of Transparent Conducting Carbon Nanotube Films. *ACS Nano* **2009**, *3*, 835–843.
47. Vigolo, B.; Penicaud, A.; Coulon, C.; Sauder, C.; Pailler, R.; Journet, C.; Bernier, P.; Poulin, P. Macroscopic Fibers and Ribbons of Oriented Carbon Nanotubes. *Science* **2000**, *290*, 1331–1334.
48. Dalton, A. B.; Collins, S.; Munoz, E.; Razal, J. M.; Ebron, V. H.; Ferraris, J. P.; Coleman, J. N.; Kim, B. G.; Baughman, R. H. Super-Tough Carbon-Nanotube Fibres—These Extraordinary Composite Fibres Can Be Woven into Electronic Textiles. *Nature* **2003**, *423*, 703.
49. Kumar, S.; Dang, T. D.; Arnold, F. E.; Bhattacharyya, A. R.; Min, B. G.; Zhang, X. F.; Vaia, R. A.; Park, C.; Adams, W. W.; Hauge, R. H.; *et al.* Synthesis, Structure, and Properties of PBO/SWNT Composites. *Macromolecules* **2002**, *35*, 9039–9043.
50. Davis, V. A.; Ericson, L. M.; Parra-Vasquez, A. N. G.; Fan, H.; Wang, Y. H.; Prieto, V.; Longoria, J. A.; Ramesh, S.; Saini, R. K.; Kittrell, C.; *et al.* Phase Behavior and Rheology of SWNTs in Superacids. *Macromolecules* **2004**, *37*, 154–160.
51. Ericson, L. M.; Fan, H.; Peng, H. Q.; Davis, V. A.; Zhou, W.; Sulpizio, J.; Wang, Y. H.; Booker, R.; Vavro, J.; Guthy, C.; *et al.* Macroscopic, Neat, Single-Walled Carbon Nanotube Fibers. *Science* **2004**, *305*, 1447–1450.
52. Ramesh, S.; Ericson, L. M.; Davis, V. A.; Saini, R. K.; Kittrell, C.; Pasquali, M.; Billups, W. E.; Adams, W. W.; Hauge, R. H.; Smalley, R. E. Dissolution of Pristine Single Walled Carbon Nanotubes in Superacids by Direct Protonation. *J. Phys. Chem. B* **2004**, *108*, 8794–8798.
53. Parra-Vasquez, A. N. G. Solubility, Length Characterization, and Cryo-TEM of Pristine and Functionalized Single-Walled Carbon Nanotubes in Surfactant and Superacid Systems, with Application to Spinning SWNT Fibers, Ph.D. Thesis, Rice University, 2009.
54. Hu, H.; Zhao, B.; Itkis, M. E.; Haddon, R. C. Nitric Acid Purification of Single-Walled Carbon Nanotubes. *J. Phys. Chem. B* **2003**, *107*, 13838–13842.
55. Zhang, X. F.; Sreekumar, T. V.; Liu, T.; Kumar, S. Properties and Structure of Nitric Acid Oxidized Single Wall Carbon Nanotube Films. *J. Phys. Chem. B* **2004**, *108*, 16435–16440.
56. Sumanasekera, G. U.; Allen, J. L.; Fang, S. L.; Loper, A. L.; Rao, A. M.; Eklund, P. C. Electrochemical Oxidation of Single Wall Carbon Nanotube Bundles in Sulfuric Acid. *J. Phys. Chem. B* **1999**, *103*, 4292–4297.
57. Flory, P. J. Statistical Thermodynamics of Semi-Flexible Chain Molecules. *Proc. R. Soc. London, Ser. A* **1956**, *234*, 60–73.
58. Green, M. J.; Parra-Vasquez, A.; Behabtu, N.; Pasquali, M. Modeling the Phase Behavior of Polydisperse Rigid Rods in Attractive Solvents, with Applications to SWNTs in Superacids. *J. Chem. Phys.* **2009**, *131*, 084901.
59. Rai, P. K.; Pinnick, R. A.; Parra-Vasquez, A. N. G.; Davis, V. A.; Schmidt, H. K.; Hauge, R. H.; Smalley, R. E.; Pasquali, M. Isotropic-Nematic Phase Transition of Single-Walled Carbon Nanotubes in Strong Acids. *J. Am. Chem. Soc.* **2006**, *128*, 591–595.
60. Onsager, L. The Effects of Shape on the Interaction of Colloidal Particles. *Ann. N.Y. Acad. Sci.* **1949**, *51*, 627–659.
61. Bandyopadhyaya, R.; Nativ-Roth, E.; Regev, O.; Yerushalmi-Rozen, R. Stabilization of Individual Carbon Nanotubes in Aqueous Solutions. *Nano Lett.* **2002**, *2*, 25–28.
62. Fagan, J. A.; Landi, B. J.; Mandelbaum, I.; Simpson, J. R.; Bajpai, V.; Bauer, B. J.; Migler, K.; Walker, A. R. H.; Raffaelle, R.; Hobbie, E. K. Comparative Measures of Single-Wall Carbon Nanotube Dispersion. *J. Phys. Chem. B* **2006**, *110*, 23801–23805.
63. Solomon, M. J.; Spicer, P. T. Microstructural Regimes of Colloidal Rod Suspensions, Gels, and Glasses. *Soft Matter* **2010**, *6*, 1391–1400.
64. Reed, C. A.; Kim, K. C.; Bolskar, R. D.; Mueller, L. J. Taming Superacids: Stabilization of the Fullerene Cations HC60+ and C60+. *Science* **2000**, *289*, 101–104.
65. Saito, R.; Dresselhaus, G.; Dresselhaus, M. S. Physical Properties of Carbon Nanotubes. *Physical Properties of Carbon Nanotubes*; Imperial College Press: London, 1998.
66. Scholte, T. G. Molecular Weights and Molecular Weight Distribution of Polymers by Equilibrium Ultracentrifugation. II. Molecular Weight Distribution. *J. Polym. Sci., Part A-2: Polym. Phys.* **1968**, *6*, 111–127.
67. Rossen, W. R.; Davis, H. T.; Scriven, L. E. Sedimentation of Molecular Solutions in the Ultracentrifuge. II. Sedimentation-Velocity. *J. Colloid Interface Sci.* **1986**, *113*, 269–287.
68. Schuck, P. Size-Distribution Analysis of Macromolecules by Sedimentation Velocity Ultracentrifugation and Lamm Equation Modeling. *Biophys. J.* **2000**, *78*, 1606–1619.
69. Arnold, M. S.; Stupp, S. I.; Hersam, M. C. Enrichment of Single-Walled Carbon Nanotubes by Diameter in Density Gradients. *Nano Lett.* **2005**, *5*, 713–718.
70. Fagan, J. A.; Becker, M. L.; Chun, J.; Hobbie, E. K. Length Fractionation of Carbon Nanotubes Using Centrifugation. *Adv. Mater.* **2008**, *20*, 1609–1613.
71. Fagan, J. A.; Becker, M. L.; Chun, J. H.; Nie, P. T.; Bauer, B. J.; Simpson, J. R.; Hight-Walker, A.; Hobbie, E. K. Centrifugal Length Separation of Carbon Nanotubes. *Langmuir* **2008**, *24*, 13880–13889.
72. Liu, T.; Luo, S. D.; Xiao, Z. W.; Zhang, C.; Wang, B. Preparative Ultracentrifuge Method for Characterization of Carbon Nanotube Dispersions. *J. Phys. Chem. C* **2008**, *112*, 19193–19202.
73. Green, M. J.; Young, C. C.; Parra-Vasquez, A. N. G.; Majumder, M.; Juloori, V.; Behabtu, N.; Schmidt, J.; Kesselman, E.; Cohen, Y.; Talmon, Y.; *et al.* Manuscript in preparation.
74. Behabtu, N.; Lomeda, J.; Green, M. J.; Higginbotham, A. L.; Sinitskii, A.; Kosynkin, D. K.; Tsentalovich, D.; Parra-Vasquez, A. N. G.; Schmidt, J.; Kesselman, E.; *et al.*

Spontaneous High-Concentration Dispersions and Liquid Crystals of Graphene. *Nat. Nanotechnol.* **2010**, *5*, 406–411.
75. Yakobson, B. I.; Samsonidze, G.; Samsonidze, G. G. Atomistic Theory of Mechanical Relaxation in Fullerene Nanotubes. *Carbon* **2000**, *38*, 1675–1680.
76. Bachilo, S. M.; Strano, M. S.; Kittrell, C.; Hauge, R. H.; Smalley, R. E.; Weisman, R. B. Structure-Assigned Optical Spectra of Single-Walled Carbon Nanotubes. *Science* **2002**, *298*, 2361–2366.
77. Parra-Vasquez, A. N. G.; Stepanek, I.; Davis, V. A.; Moore, V. C.; Haroz, E. H.; Shaver, J.; Hauge, R. H.; Smalley, R. E.; Pasquali, M. Simple Length Determination of Single-Walled Carbon Nanotubes by Viscosity Measurements in Dilute Suspensions. *Macromolecules* **2007**, *40*, 4043–4047.
78. Pint, C. L.; Pheasant, S. T.; Parra-Vasquez, A. N. G.; Horton, C.; Xu, Y. Q.; Hauge, R. H. Investigation of Optimal Parameters for Oxide-Assisted Growth of Vertically Aligned Single-Walled Carbon Nanotubes. *J. Phys. Chem. C* **2009**, *113*, 4125–4133.
79. Ci, L.; Manikoth, S. M.; Li, X.; Vajtai, R.; Ajayan, P. M. Ultra-Thick Freestanding Aligned Carbon Nanotube Films by a Self-Releasing Technique. *Adv. Mater.* **2007**, *19*, 3300–3307.